Journal of Physiology (1992), **445**, *pp.* 141–156
With 9 figures
Printed in Great Britain

MEMBRANE CURRENTS IN SMALL CULTURED RAT HIPPOCAMPAL NEURONS: A VOLTAGE-CLAMP STUDY

BY STAFFAN JOHANSSON* AND PETER ÅRHEM

From the Nobel Institute for Neurophysiology, Karolinska Institutet, S-104 01 Stockholm, Sweden

(*Received 15 January 1991*)

SUMMARY

1. The currents underlying the graded impulses in small cultured hippocampal neurons from rat embryos were analysed under voltage-clamp conditions with the tight-seal whole-cell recording technique.

2. The leak and capacitative currents induced by a potential step were linearly related to the potential in the range studied (−60 to −100 mV).

3. With steps to potentials more positive than −40 mV, at least two different potential-activated currents were detected: an initial transient current and a delayed sustained one. In addition, 40% of the cells studied showed a delayed transient current.

4. The initial transient current showed sigmoid activation and roughly exponential inactivation. Its reversal potential depended on the Na^+ concentration and was close to the Na^+ equilibrium potential. Further, it was blocked by 3·0 μM-tetrodotoxin, and was abolished when choline was substituted for Na^+ in the extracellular solution. We concluded that this current was carried mainly by Na^+ ions.

5. The delayed sustained current showed sigmoid activation and almost no inactivation within 40 ms. The reversal potential was close to the K^+ equilibrium potential. We concluded that this current was carried mainly by K^+ ions.

6. The delayed transient current was outward in the potential range studied (−50 to +120 mV) and did not depend on the pipette Cl^- concentration. It was assumed that this current was carried mainly by K^+ ions.

7. A quantitative description of the initial transient and the delayed sustained currents was developed on the basis of earlier descriptions of excitable membranes.

INTRODUCTION

In a previous paper (Johansson, Friedman & Århem, 1992) we described the unexpected finding that small cultured hippocampal neurons from rat embryos generate action potentials with an amplitude and time course that strongly depend on stimulus strength. This implied a deviation from the 'all-or-nothing' principle and

* To whom correspondence should be addressed.

MS 9078

prompted an investigation of the currents underlying the potential response. The mechanism underlying graded impulses in other systems has been debated. For instance, modified Na^+ channel gating and persistent activation of K^+ channels have been proposed (Bush, 1981).

The present paper describes the currents in cultured hippocampal neurons as revealed by voltage-clamp analysis. To compute action potentials of the cells studied (Johansson & Århem, 1992), we describe the currents quantitatively. The description of the membrane of the node of Ranvier in amphibian nerve fibres (Frankenhaeuser, 1960, 1963; Frankenhaeuser & Huxley, 1964) was used with minor modifications. Some preliminary results of this study have been published (Johansson & Århem, 1990).

METHODS

Cell culture conditions

The cells were prepared from embryonic rat hippocampi, using the techniques described in the preceding paper (Johansson *et al.* 1992).

Electrophysiological recordings and treatment of data

The currents described in this paper were recorded under voltage-clamp conditions with the tight-seal whole-cell method (Marty & Neher, 1983). The recording technique and equipment were similar to those described in the previous paper (Johansson *et al.* 1992). All recordings were performed at room temperature (21–23 °C).

Leak and capacitative currents were subtracted on the assumption of a linear current–potential relation (see Results). For the procedure, we used the currents associated with small negative potential steps: either the currents directly or a curve described by the sum of two or three exponential terms (and an offset constant) fitted to the current. Since the current values were multiplied by scaling factors before subtraction, the former method artifactually increased noise in the current records (see Figs 1 and 4*A* and *B*), while the latter method kept the noise at the original level (see Figs 5, 6*A* and 7*A*).

The curves fitted to the recorded currents were generated with the pCLAMP program (Axon Instruments, USA), based on algorithms minimizing the least-squares error between data points and calculated fit points.

The space-clamp conditions seemed appropriate in most cells. This was concluded from the analysis of the potential-activated currents, and the finding of 'regenerative' inward currents in a few cells (see Results and Discussion).

Due to the multi-exponential time course of the capacitative and leak currents (see Results), no value for the series resistance of the pipette–cell pathway was obtained (cf. Fenwick, Marty & Neher, 1982*a*). To reduce the potential error introduced by the series resistance, the detailed quantitative analysis was restricted to measurements made with 2 MΩ pipettes. Assuming the series resistance to be twice the resistance of the open pipette (Marty & Neher, 1983), the expected potential error would be 4 mV for a current of 1000 pA, and less for most recorded currents.

The membrane-specific values given in parentheses in the text are based on an estimated mean membrane area of 200 μm^2 (Johansson *et al.* 1992), unless otherwise stated.

Solutions

The cells were bathed in a standard solution containing (in mM): 137 NaCl, 5·0 KCl, 1·0 $CaCl_2$, 1·2 $MgCl_2$ and 10 HEPES (*N*-(2-hydroxyethyl)piperazine-*N'*-2-ethanesulphonic acid), pH 7·4. In a few experiments, 5 mM-D-glucose was added to this solution. No systematic difference between cells in solutions with or without glucose was observed. As pipette filling solution, one of the following solutions was used (in mM): (I) 140 KCl, 3·0 NaCl, 1·2 $MgCl_2$, 1·0 EGTA (ethyleneglycol-bis-(*β*-aminoethylether)*N,N,N',N'*-tetraacetic acid) and 10 HEPES, pH 7·2; or (II) 140 KOH/KH_2PO_4, 3·0 NaCl, 1·2 $MgCl_2$, 1·0 EGTA and 3·0 Na_2-ATP, pH 7·2. Concentrations are given in the text with the ion species in square brackets and subscripts for inside (i) or outside (o) of the membrane.

RESULTS

The currents associated with rectangular potential steps were recorded and analysed. To reduce possible potential-dependent inactivation of currents as described for other excitable membranes (e.g. Hodgkin & Huxley, 1952*b*;

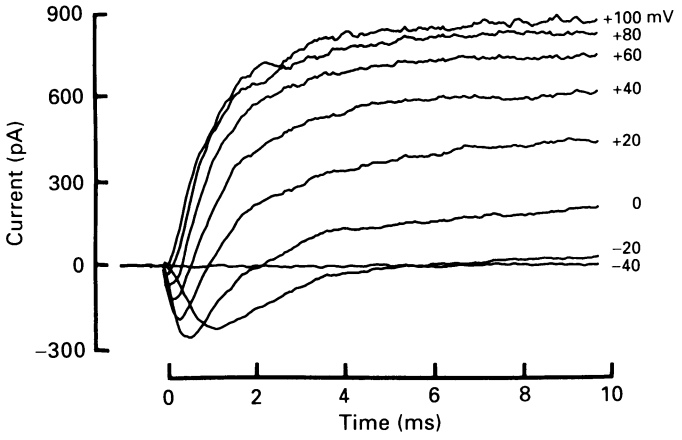

Fig. 1. Current responses to rectangular potential steps. Holding potential was −70 mV, and step potentials varied from −40 to +100 mV, as indicated. Leak and capacitative currents were subtracted. Remaining transients due to imperfect subtraction were truncated.

Frankenhaeuser, 1959), the membrane potential between the test steps was in most experiments held somewhat more negative than the resting potential. A typical family of currents is shown in Fig. 1. As with other excitable membranes, we could distinguish potential-activated current components as well as leak and capacitative components.

Capacitative and leak currents

The capacitative (I_C) and the leak (I_L) current transport mechanisms were studied by applying negative (Fig. 2*A*) or small positive potential steps. The time course of current following the peak could not be described by a single exponential function. A sum of two or three exponentials was needed for a reasonable fit (Fig. 2*B*).

The current was linearly related to the potential in the range from −60 to −100 mV (Fig. 2*C*). This relation applied to the whole time range studied (from 0·2 to more than 20 ms after the onset of the potential step).

The input resistance derived from the steady-state current (measured at more than 20 ms after the onset of the pulse in order to avoid slow capacitative components) for thirteen cells was 3·6 ± 2·3 GΩ (mean ± standard deviation; about 7·2 kΩ cm^2). This is close to the value (3·3 ± 1·4 GΩ) obtained under current-clamp conditions (Johansson *et al.* 1992).

Potential-activated currents

In twelve of twenty cells studied, in the range from −20 mV (usually above −40 mV) to about +100 mV, an initial transient inward current was followed by a

delayed sustained outward current (Fig. 1). The latter showed negligible inactivation for pulse durations up to 40 ms. The remaining eight cells showed, in addition, an outward transient current, resulting in an outward peak followed by a decline to a steady current level (Figs 5 and 7*A*). All the cells tested in this study generated

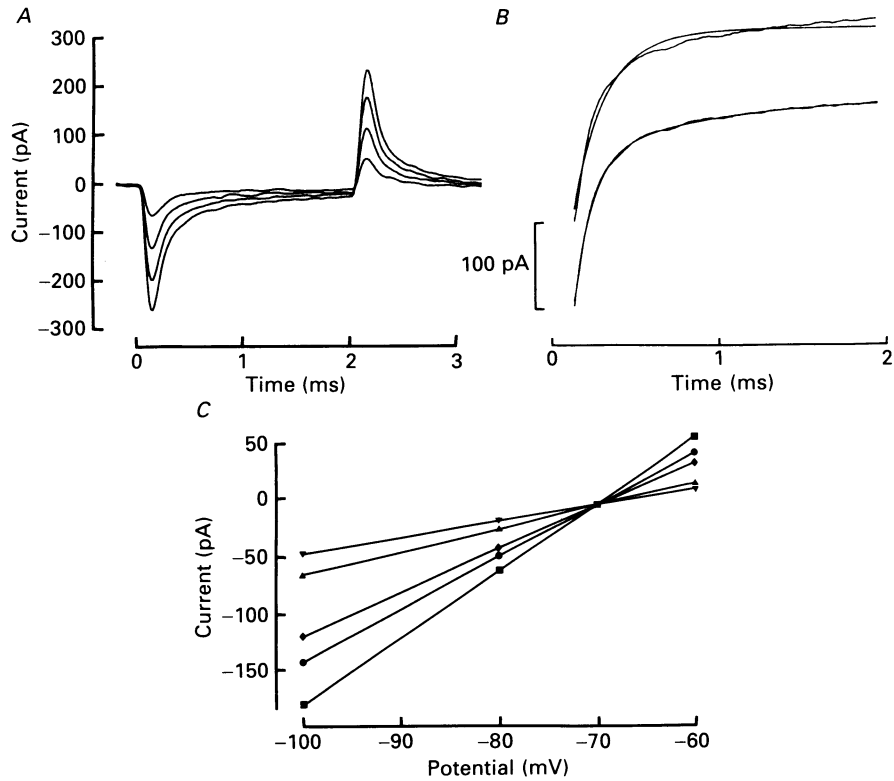

Fig. 2. Capacitative and leak currents. *A*, responses to 2 ms, negative rectangular potential steps. Note the fast timescale. Holding potential was −60 mV, and step potentials were (from top to bottom) −65, −70, −75 and −80 mV. *B*, multi-exponential current decay. The time course of the largest current response shown in *A* (for times between 0·15 and 1·95 ms) was fitted with the sum of a constant and one exponential term (upper curves; time constant 0·20 ms) or the sum of a constant and two exponential terms (lower curves; time constants 0·11 and 0·77 ms). *C*, current–potential relation for capacitative and leak currents. Currents were measured at 0·3 (■), 0·4 (●), 0·5 (◆), 1·0 (▲) and 1·5 ms (▼) after the onset of a rectangular potential step. The neighbouring points for each time are connected by straight lines. Note the linearity. Holding potential was −70 mV. (A different cell than for *A* and *B*.)

graded action potentials (Johansson *et al.* 1992) irrespective of whether a transient outward current was present.

Initial transient current

The initial transient current showed a sigmoid activation phase and a slower, roughly mono-exponential inactivation phase (e.g. Fig. 4*B*). Activation and inactivation were both faster at more positive potentials (Figs 1 and 7*A*). The

current peak plotted against the membrane potential is shown in Fig. 3*A* (●), for pipette solution I (see Methods). Here, the current was activated exclusively at potentials more positive than −40 mV. In other cells, the current was activated above a lowest potential value ranging between −50 and −20 mV. The current

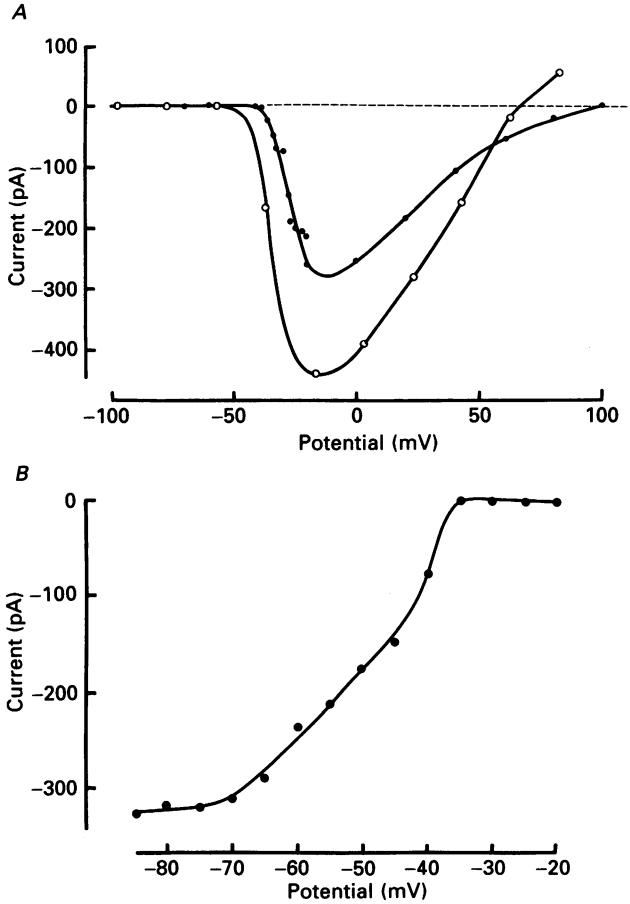

Fig. 3. Current–potential relations for the initial transient current. *A*, peak of initial transient current. ●, pipette solution I ($[Na^+]_i$ = 3·0 mM). Holding potential was −70 mV. Note the reversal potential just below +100 mV. ○, pipette solution II ($[Na^+]_i$ = 9·0 mM). Holding potential was −97 mV. Note the reversal potential at about +67 mV. Different cells were used for the two curves. ($[Na^+]_o$ = 137 mM for both curves.) *B*, inactivation curve for the initial transient current. The peak of the initial transient current at a potential step to 0 mV was plotted against the potential of a 50 ms preceding step. Holding potential was −70 mV. Potential for half-maximal current was about −45 mV. I_C and I_L were subtracted (*A* and *B*).

reversed from inward to outward slightly below +100 mV. This is close to the expected equilibrium potential for Na^+, which in this case is +97 mV ($[Na^+]_o$ = 137 mM and $[Na^+]_i$ = 3·0 mM). When pipette solution II ($[Na^+]_i$ = 9·0 mM) was used, similar currents were elicited, but with a reversal potential close to +70 mV (Fig. 3*A*, ○). The expected equilibrium potential for Na^+ is in this case +69 mV.

The maximum (negative) inward peak current elicited from a holding potential of −70 mV ranged from −100 pA (about 50 μA cm^{-2}) to −1554 pA (about 780 μA cm^{-2}) in nineteen different cells (mean value −361 pA; about 180 μA cm^{-2}; leak and capacitative components subtracted).

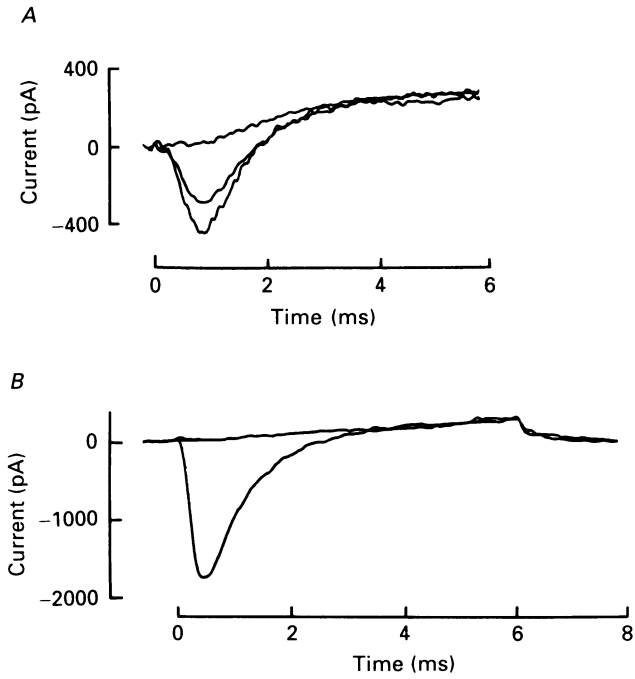

Fig. 4. Experiments on the selectivity of the initial current. *A*, effects of a Na^+-free solution. Current responses to a potential step from −75 to −5 mV before (lower curve) and after (upper curve) the substitution of choline for Na^+ in the external solution. The middle curve shows the reappearance of the inward current in the Na^+-containing solution after wash-out of choline. *B*, effects of TTX. Current responses to a 6 ms potential step from −80 mV to −10 mV before (lower curve) and after (upper curve) 3·0 μM-TTX was added to the external solution. (Note the exceptionally large current.) I_C and I_L were subtracted (*A* and *B*).

The current was partly inactivated at the resting potential. An inactivation curve, constructed from the peak current values at 0 mV *versus* the potential of a preceding conditioning pulse of 50 ms duration, is shown in Fig. 3*B*. (Fifty millisecond conditioning pulses were sufficient for the inactivation to reach a steady-state value.) The potential for half-inactivation ranged between −42 and −60 mV for six cells.

The reversal potentials with pipette solutions I and II, described above, suggested that the initial current was carried mainly by Na^+ ions. Further evidence for this was obtained from experiments using choline instead of Na^+ in the extracellular solution (cf. Hodgkin & Huxley, 1952*a*). This procedure reversibly abolished the inward initial current (Fig. 4*A*). The reversal potential of the initial peak was gradually shifted in the negative direction during the solution exchange to the Na^+-free solution.

Addition of the selective Na^+ channel blocker tetrodotoxin (TTX, 3·0 μM; Narahashi, Moore & Scott, 1964; see also Hille, 1984) to the extracellular solution completely blocked the initial current (Fig. 4*B*, see also Fig. 6*A*). This effect was only partly reversible within the 5 min studied after washing with TTX-free solution.

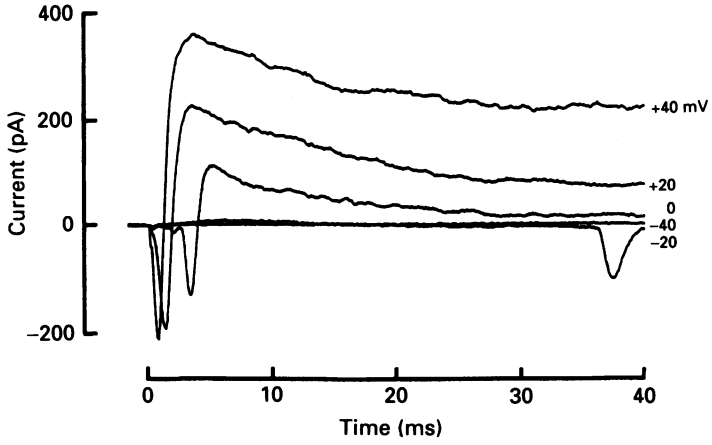

Fig. 5. Regenerative inward current component and delayed transient currents. Current responses to potential steps to indicated values from a holding potential of −70 mV. Note the submaximal regenerative inward current at the step to −20 mV. I_C and I_L were subtracted.

'Regenerative' inward current

In seven (about 35%) of the cells studied, an additional inward current was observed (Fig. 5). This differed from the initial current described above by a delayed onset and a sharp threshold in the potential range −50 to −20 mV. The delay varied with potential, sometimes exceeding 35 ms just above threshold (Fig. 5).

This 'regenerative' current usually interfered with the initial transient current. We could not, however, find any systematic interference between the regenerative inward current and either of the types of delayed current described below; nor could we find any clear difference between the potential responses (Johansson *et al.* 1992) to current steps in cells with or without the regenerative current component.

Delayed sustained current

The delayed sustained current (Fig. 1) was observed in isolation when TTX was added to the external solution (Fig. 6*A*). It was activated in the same potential range as the early transient current (i.e. above about −40 mV). The activation, which was sigmoid, was faster at increased positive potential steps. However, even at small steps, a steady or very slowly changing current level was reached within 5–15 ms of the step onset. In cells with a delayed transient current, the time was usually longer. The steady-state current amplitude plotted against potential is exemplified in Fig. 6*B*. At high potential values the current showed rectification (i.e. the slope of the current–potential curve decreased).

The maximum outward current, as measured at +60 mV when elicited from a holding potential of −70 mV, ranged from 200 pA (about 100 μA cm^{-2}) to 1240 pA

(about 620 μA cm^{-2}) in eighteen different cells (mean value 533 pA; about 270 μA cm^{-2}). These values include the delayed transient current described below, but not the leak and capacitative components.

The current was outward in the whole potential range for activation (above about −40 mV; studied up to +120 mV) and showed the same pattern with pipette

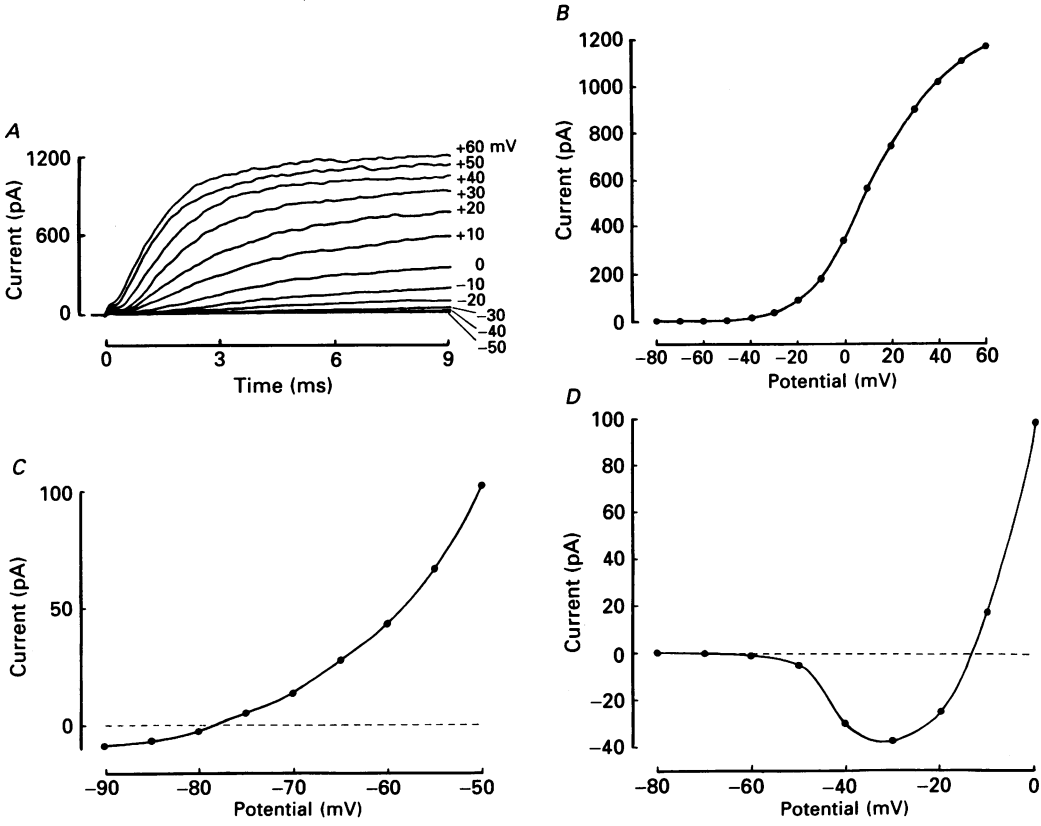

Fig. 6. Delayed sustained current. TTX (3·0 μM) was included in the external solution. *A*, current responses to potential steps to indicated values from a holding potential of −70 mV. *B*, current–potential relation for the delayed sustained current at the end of the records shown in *A*. *C*, tail-current–potential relation for the delayed sustained current. The current was measured 4·5 ms after the end of a preceding potential step to +60 mV. *D*, current–potential relation for the delayed sustained current. The K^+ concentration in the external solution was 93 mM and the Na^+ concentration 49 mM. I_C and I_L were subtracted (*A–D*).

solutions I or II, containing 145 and 5·4 mM-Cl^- respectively. The reversal potential was obtained from the tail currents after the end of a rectangular positive activating potential step (Fig. 6*C*; cf. Fig. 4*B* at time > 6 ms). It varied between −75 and −83 mV. The estimated equilibrium potential for K^+ was −85 mV ($[K^+]_o$ = 5·0 mM and $[K^+]_i$ = 140 mM). When the K^+ and Na^+ concentrations in the external solution were changed to 93 and 49 mM respectively (pipette solution II and 3·0 μM-TTX in the external solution), the current induced by low positive potential steps became

inward, and reversed at about −15 mV (Fig. 6*D*). The estimated equilibrium potential for K^+ was in this case −10 mV. Thus, we assumed that the current was carried mainly by K^+ ions.

Delayed transient current

A delayed transient outward current was seen in eight of twenty cells (Figs 5 and 7*A*). In some, it was most evident at large positive potential steps (Fig. 7*A*), but in others it was also clearly seen at small steps (Fig. 5). It was, however, never seen at steps to values below −50 mV. The amplitude at high potential values (> +40 mV) exceeded that of the steady outward current by up to 80%, when elicited from a holding potential of −70 mV. The current showed some steady-state inactivation at −70 mV and could be increased by keeping the holding potential at more negative values (Fig. 7*B*). We therefore tested ten cells that did not show a delayed transient current at a holding potential of −70 mV for the presence of this current at −90 mV or below. No such current was found here, nor when TTX (3·0 μM) was used to eliminate a possible Na^+ current interference (two cells).

The delayed transient current was, like the delayed sustained current, outward in the potential range −50 to +120 mV when standard extracellular solution was used (see Methods), and showed the same pattern with pipette solutions I or II. We therefore assumed that this component was carried mainly by K^+ ions.

Quantitative description of the currents

Our aim was to analyse the ion currents underlying the graded potential responses described in a previous paper (Johansson *et al.* 1992). To compute the potential response for the cells studied (described in a subsequent paper, Johansson & Århem, 1992), a detailed description of the initial transient current and the delayed sustained current was needed. The delayed transient current was not quantified, since graded action potentials were also generated in cells without this current component. As a basis for the description we used the equations developed by Hodgkin & Huxley (1952*c*) with the modifications introduced by Frankenhaeuser (1960, 1963; see also Frankenhaeuser & Huxley, 1964) for the nodal membrane in the myelinated vertebrate axon.

The assumptions, symbols and equations are described in the Appendix. In short, we assume that the initial transient current corresponds to the nodal Na^+ current, and the delayed sustained current to the nodal K^+ current; further we describe the currents in terms of the permeability constants $\bar{P}_{Na}$ and P'_K, and the dimensionless variables m, h and n, which are functions of potential-dependent but time-independent rate constants.

The exponents in the formulations hm^2 and n^2 (eqns (2) and (6), Appendix) were determined from double-logarithmic plots of the time course of the recorded currents. The rate constants were determined by a repeated comparative procedure in which the constants A, B and C (eqns (8)–(13)) were adjusted to obtain a good fit between computed and recorded currents. The permeability constants $\bar{P}_{Na}$ and P'_K were then chosen to give the correct current magnitude.

Figure 8 shows computed current responses to various potential steps, with parameters chosen to fit the experimentally recorded currents shown in Fig. 1. The

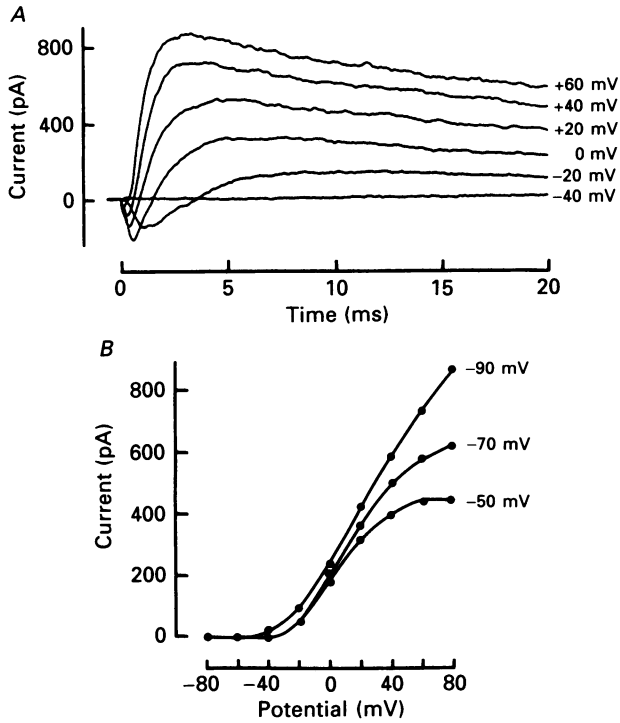

Fig. 7. Delayed transient current. *A*, current responses to potential steps to indicated values. Note that initial transient, delayed sustained and delayed transient components are present. *B*, peak-current–potential relation for the delayed transient current (delayed sustained component included). The cell membrane was held at different potentials, as indicated, before and between the test steps. Data from different cells in *A* and *B*. I_C and I_L were subtracted (*A* and *B*).

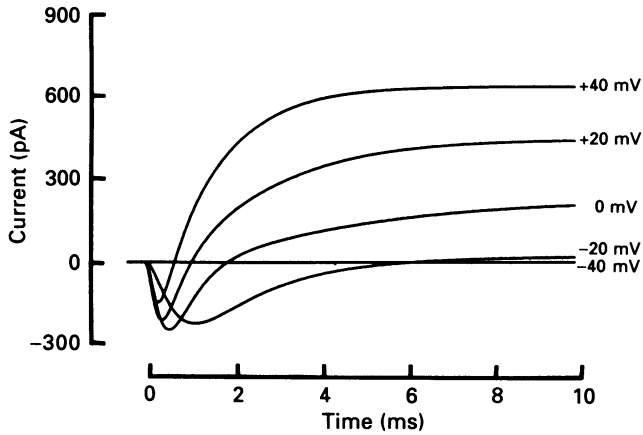

Fig. 8. Computed currents in response to rectangular potential steps. Parameter values were chosen to fit the observed currents in Fig. 1. Step potential values were as indicated. Holding potential was -70 mV. $\bar{P}_{Na}$ was $1{\cdot}3 \times 10^{-4}$ cm s^{-1} and P'_K $2{\cdot}4 \times 10^{-5}$ cm s^{-1}. Estimated membrane area was 100 μm^2.

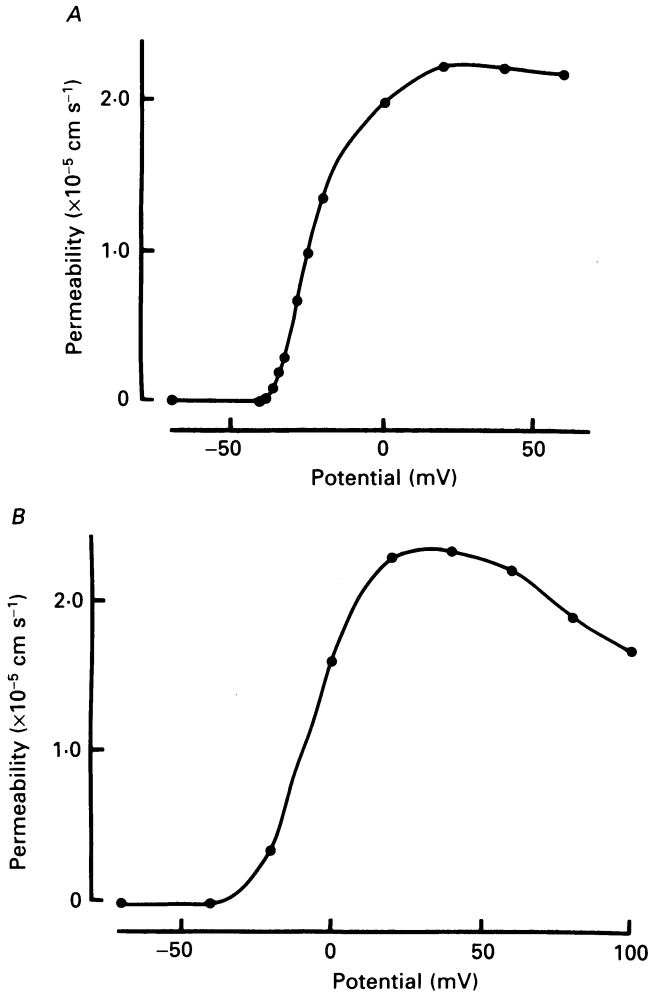

Fig. 9. Permeability–potential relations. *A*, permeability at the peak of the initial transient current (cf. Fig. 3*A*). Calculation assumed a Na^+ selectivity. *B*, permeability at steady state of the delayed sustained current. Calculation assumed a K^+ selectivity. Note the decrease in permeability at high potentials. Estimated membrane area of this cell was 100 μm^2.

TABLE 1. Constants used for the calculation of rate constants (see text)

		α_h	β_h	α_m	β_m	α_n	β_n
A	(mV^{-1} ms^{-1})	0·05	2·25*	0·06	0·07	0·016	0·04
B	(mV)	5	60	37	28	60	35
C	(mV)	6	10	3	20	10	10

*, (ms^{-1})

values for the constants A, B and C are given in Table 1. $\bar{P}_{Na}$ and P'_K were $1{\cdot}3 \times 10^{-4}$ and $2{\cdot}4 \times 10^{-5}$ cm s^{-1} respectively.

Permeabilities associated with the recorded currents

On the assumptions described above (and in the Appendix) and after an estimation of the membrane area (see Johansson *et al.* 1992), the permeabilities associated with the initial transient and the delayed sustained current were calculated (from eqns (1) and (5) in the Appendix).

Figure 9*A* shows the calculated peak permeability for the initial transient current, plotted against membrane potential. As can be seen, permeability increased with potential in the range -40 mV to about $+20$ mV. The estimated maximum permeability (at the peak of the initial current) varied between 2×10^{-6} and 3×10^{-5} cm s^{-1} in the different cells.

Figure 9*B* shows the calculated steady-state permeability for the delayed sustained current, plotted against potential (same cell as for Fig. 9*A*). Permeability increased with potential in the range -40 to about $+20$ mV, and decreased at potentials above $+40$ mV.

DISCUSSION

The present voltage-clamp analysis demonstrated that the currents of small neurons from the hippocampus of rat embryos show features similar to those described for other excitable membranes. Thus, no other potential-activated current than the initial transient current and the delayed sustained current is required for generating the graded action potentials described for these cells (Johansson *et al.* 1992). We made no attempt to separate the currents further into different contributing components.

For several reasons (reversal potential, kinetics and its potential dependence, effects of TTX and substitution of choline for Na^+ in the extracellular solution) it seems likely that the initial transient current was an ordinary Na^+ current (Hodgkin & Huxley, 1952*a*; Dodge & Frankenhaeuser, 1959; Barrett & Crill, 1980). For similar reasons (reversal potential, kinetics and its potential dependence, independence of pipette Cl^- concentration), the delayed sustained current was most likely a delayed K^+ one (Hodgkin & Huxley, 1952*a*; Frankenhaeuser, 1962; Barrett, Barrett & Crill, 1980) and the delayed transient current an 'A-type' K^+ current (Hagiwara, Kusano & Saito, 1961; Connor & Stevens, 1971; Neher, 1971; Gustafsson, Galvan, Grafe & Wigström, 1982). The A current was found in fewer than half the cells (eight of twenty). The reason for this is unclear: perhaps different types of cell or cells at different developmental stages. However, graded action potentials were also seen in cells without an A current, implying that the A current is not required for the generation of graded action potentials.

Comparison with other cells

Some differences between our measurements and others reported in the literature were noted. Our currents were considerably smaller than those found in axons (Hodgkin & Huxley, 1952*a*: Dodge & Frankenhaeuser, 1959; Frankenhaeuser, 1962), and smaller than the outward currents studied in larger hippocampal

pyramidal and multipolar neurons (soma diameter 15–20 μm; Segal & Barker, 1984), but closer to those in somewhat smaller pyramidal neurons (soma about 7–12 μm; Numann, Wadman & Wong, 1987). Further, they seem to be of the same order of magnitude as those recorded in the somata of other small excitable cells (Fenwick, Marty & Neher, 1982*b*; Hockberger, Tseng & Connor, 1987; Cull-Candy, Marshall & Ogden, 1989; Johansson, Rydqvist, Swerup, Heilbronn & Århem, 1989). Note also that several studies indicate an increase in Na^+ channel density during development (MacDermott & Westbrook, 1986; Huguenard, Hamill & Prince, 1988).

Another difference concerns the time course of I_C and I_L. The response to small or negative potential steps did not show a simple exponential decay. This is in contrast to chromaffin cells of the adrenal medulla (Fenwick *et al.* 1982*a*). Resistances and capacitances in neurites, which are not present in the chromaffin cells, are likely to contribute to the more complex time course seen in the present study.

A third difference between the present findings and earlier ones concerns the linearity of the leak current–potential relation. Where our measurements showed a clear linearity in the range -60 to -100 mV, a non-linear relation in the potential range -60 to -150 mV has been reported for chromaffin cells (Fenwick *et al.* 1982*a*). On the other hand, the amphibian node of Ranvier shows a linear relation (Dodge & Frankenhaeuser, 1959). The reason for this discrepancy is unknown.

Concerning the 'regenerative' inward currents, similar currents have been recorded in other preparations (e.g. Århem, Frankenhaeuser & Moore, 1973; Barrett & Crill, 1980; Hockberger *et al.* 1987; Huguenard *et al.* 1988). In these cases the currents were assumed to result from insufficient voltage-clamp control. This is probably also the case in the present study, since full voltage-clamp control cannot be expected in the neurites, due to intraneuritic series resistances. Since most cells did not show this current component, it is not likely that poor space-clamp conditions constituted a major problem.

Quantitative description of the potential-activated currents

We chose to base our quantitative description of the potential-activated currents on that of Frankenhaueser & Huxley (1964) for myelinated nerve fibres from *Xenopus laevis*, since this preparation has been analysed in great detail. After appropriate parameter modifications, the equations used were judged adequate for our purpose of phenomenological description. In a subsequent paper (Johansson & Århem, 1992), we will show that the equations obtained can be used to compute potential responses similar to those observed experimentally.

APPENDIX

Mathematical treatment of data

The mathematical treatment of the currents closely follows the description of the membrane of the node of Ranvier in amphibian myelinated nerve fibres (Frankenhaeuser, 1960, 1963; Frankenhaeuser & Huxley, 1964). The following assumptions were made: (i) the initial transient current is carried by Na^+; (ii) the delayed sustained current is carried by K^+; (iii) the Na^+ and K^+ currents follow the constant-

field equation; (iv) the Na^+ and K^+ permeabilities depend on membrane potential and time (see Goldman, 1943; Hodgkin & Katz, 1949; Frankenhaeuser 1960, 1963).

List of symbols

U: membrane potential;
U_R: resting or holding potential;
I_{Na}: initial transient current;
I_K: delayed sustained current;
P_{Na}, P_K: permeabilities for I_{Na} and I_K;
$\bar{P}_{Na}$, P'_K: permeability constants (see equations);
m, h, n: permeability variables for P_{Na} activation (m), inactivation (h) and P_K activation (n);
α, β: rate constants for m, h and n as indicated by suffix;
A, B, C: empirical constants in eqns (8)–(13) for αs and βs (given in Table 1);
A_m: membrane area;
R: gas constant;
F: Faraday's constant;
T: absolute temperature;
t: time.

Equations

$$I_{Na} = A_m P_{Na} \frac{UF^2}{RT} \frac{[Na^+]_o - [Na^+]_i \exp(UF/RT)}{1-\exp(UF/RT)}, \tag{1}$$

$$P_{Na} = \bar{P}_{Na} h m^2, \tag{2}$$

$$dm/dt = \alpha_m (1-m) - \beta_m m, \tag{3}$$

$$dh/dt = \alpha_h (1-h) - \beta_h h, \tag{4}$$

$$I_K = A_m P_K \frac{UF^2}{RT} \frac{[K^+]_o - [K^+]_i \exp(UF/RT)}{1-\exp(UF/RT)}, \tag{5}$$

$$P_K = P'_K n^2, \tag{6}$$

$$dn/dt = \alpha_n (1-n) - \beta_n n. \tag{7}$$

The temperature value used in the computations is 295 K (22 °C), in order to match the experimental situation. αs and βs are described by the following equations, with the values for A, B and C (changed from those of Frankenhaeuser & Huxley, 1964) given in Table 1.

$$\alpha_m = A((U-U_R)-B)/(1-\exp((B-(U-U_R))/C)), \tag{8}$$

$$\beta_m = A(B-(U-U_R))/(1-\exp(((U-U_R)-B)/C)), \tag{9}$$

$$\alpha_h = A(B-(U-U_R))/(1-\exp(((U-U_R)-B)/C)), \tag{10}$$

$$\beta_h = A/(1+\exp((B-(U-U_R))/C)), \tag{11}$$

$$\alpha_n = A((U-U_R)-B)/(1-\exp((B-(U-U_R))/C)), \tag{12}$$

$$\beta_n = A(B-(U-U_R))/(1-\exp(((U-U_R)-B)/C)), \tag{13}$$

The numerical computations were performed on an IBM-compatible personal computer (80286 CPU) with software written in BASIC.

We thank Dr Wilma Friedman, Department of Medical Chemistry II, Karolinska Institutet, Stockholm, for providing the cell cultures, and Professor B. Frankenhaeuser and Professor S. Grillner for valuable discussions. This work was supported by grants from the Swedish Medical Research Council (project No. 6552) and Karolinska Institutets Fonder.

REFERENCES

ÅRHEM, P., FRANKENHAEUSER, B. & MOORE, L. E. (1973). Ionic currents at resting potential in nerve fibres from Xenopus laevis. Potential clamp experiments. *Acta Physiologica Scandinavica* **88**, 446–454.

BARRETT, E. F., BARRETT, J. N. & CRILL, W. E. (1980). Voltage-sensitive outward currents in cat motoneurones. *Journal of Physiology* **304**, 251–276.

BARRETT, J. N. & CRILL, W. E. (1980). Voltage clamp of cat motoneurone somata: properties of the fast inward current. *Journal of Physiology* **304**, 231–249.

BUSH, B. M. H. (1981). Non-impulsive stretch receptors in crustaceans. In *Neurons without Impulses*, ed. ROBERTS, A. & BUSH, B. M. H., pp. 147–176. Cambridge University Press, Cambridge.

CONNOR, J. A. & STEVENS, C. F. (1971). Voltage clamp studies of a transient outward membrane current in gastropod neural somata. *Journal of Physiology* **213**, 21–30.

CULL-CANDY, S. G., MARSHALL, C. G. & OGDEN, D. (1989). Voltage-activated membrane currents in rat cerebellar granule neurones. *Journal of Physiology* **414**, 179–199.

DODGE, F. A. & FRANKENHAEUSER, B. (1959). Sodium currents in the myelinated nerve fibre of *Xenopus laevis* investigated with the voltage clamp technique. *Journal of Physiology* **148**, 188–200.

FENWICK, E. M., MARTY, A. & NEHER, E. (1982*a*). A patch-clamp study of bovine chromaffin cells and of their sensitivity to acetylcholine. *Journal of Physiology* **331**, 577–597.

FENWICK, E. M., MARTY, A. & NEHER, E. (1982*b*). Sodium and calcium channels in bovine chromaffin cells. *Journal of Physiology* **331**, 599–635.

FRANKENHAEUSER, B. (1959). Steady state inactivation of sodium permeability in myelinated nerve fibres of *Xenopus laevis*. *Journal of Physiology* **148**, 671–676.

FRANKENHAEUSER, B. (1960). Quantitative description of sodium currents in myelinated nerve fibres of *Xenopus laevis*. *Journal of Physiology* **151**, 491–501.

FRANKENHAEUSER, B. (1962). Delayed currents in myelinated nerve fibres of *Xenopus laevis* investigated with voltage clamp technique. *Journal of Physiology* **160**, 40–45.

FRANKENHAEUSER, B. (1963). A quantitative description of potassium currents in myelinated nerve fibres of *Xenopus laevis*. *Journal of Physiology* **169**, 424–430.

FRANKENHAEUSER, B. & HUXLEY, A. F. (1964). The action potential in the myelinated nerve fibre of *Xenopus laevis* as computed on the basis of voltage clamp data. *Journal of Physiology* **171**, 302–315.

GOLDMAN, D. E. (1943). Potential, impedance, and rectification in membranes. *Journal of General Physiology* **27**, 37–60.

GUSTAFSSON, B., GALVAN, M., GRAFE, P. & WIGSTRÖM, H. (1982). A transient outward current in a mammalian central neurone blocked by 4-aminopyridine. *Nature* **299**, 252–254.

HAGIWARA, S., KUSANO, K. & SAITO, N. (1961). Membrane changes of *Onchidium* nerve cell in potassium-rich media. *Journal of Physiology* **155**, 470–489.

HILLE, B. (1984). *Ionic Channels of Excitable Membranes*. Sinauer, Sunderland, MA, USA.

HOCKBERGER, P. E., TSENG, H.-Y. & CONNOR, J. A. (1987). Immunocytochemical and electrophysiological differentiation of rat cerebellar granule cells in explant cultures. *Journal of Neuroscience* **7**, 1370–1383.

HODGKIN, A. L. & HUXLEY, A. F. (1952*a*). Currents carried by sodium and potassium ions through the membrane of the giant axon of *Loligo*. *Journal of Physiology* **116**, 449–472.

HODGKIN, A. L. & HUXLEY, A. F. (1952*b*). The dual effect of membrane potential on sodium conductance in the giant axon of *Loligo*. *Journal of Physiology* **116**, 497–506.

HODGKIN, A. L. & HUXLEY, A. F. (1952*c*). A quantitative description of membrane current and its application to conduction and excitation in nerve. *Journal of Physiology* **117**, 500–544.

HODGKIN, A. L. & KATZ, B. (1949). The effect of sodium ions on the electrical activity of the giant axon of the squid. *Journal of Physiology* **108**, 37–77.

HUGUENARD, J. R., HAMILL, O. P. & PRINCE, D. A. (1988). Developmental changes in Na^+ conductances in rat neocortical neurons: Appearance of a slowly inactivating component. *Journal of Neurophysiology* **59**, 778–795.

JOHANSSON, S. & ÅRHEM, P. (1990). Graded action potentials in small cultured rat hippocampal neurons. *Neuroscience Letters* **118**, 155–158.

JOHANSSON, S. & ÅRHEM, P. (1992). Computed potential responses of small cultured rat hippocampal neurons. *Journal of Physiology* **445**, 157–167.

JOHANSSON, S., FRIEDMAN, W. & ARHEM, P. (1992). Impulses and resting membrane properties of small cultured rat hippocampal neurons. *Journal of Physiology* **445**, 129–140.

JOHANSSON, S., RYDQVIST, B., SWERUP, C., HEILBRONN, E. & ÅRHEM, P. (1989). Action potentials of cultured human oat cells: whole-cell measurements with the patch-clamp technique. *Acta Physiologica Scandinavica* **135**, 573–578.

MACDERMOTT, A. B. & WESTBROOK, G. L. (1986). Early development of voltage-dependent sodium currents in cultured mouse spinal cord neurons. *Developmental Biology* **113**, 317–326.

MARTY, A. & NEHER, E. (1983). Tight-seal whole-cell recording. In *Single-Channel Recording*, ed. SAKMANN, B. & NEHER, E., pp. 107–122. Plenum Press, New York.

NARAHASHI, T., MOORE, J. W. & SCOTT, W. R. (1964). Tetrodotoxin blockage of sodium conductance increase in lobster giant axons. *Journal of General Physiology* **47**, 965–974.

NEHER, E. (1971). Two fast transient current components during voltage clamp on snail neurons. *Journal of General Physiology* **58**, 36–53.

NUMANN, R. E., WADMAN, W. J. & WONG, R. K. S. (1987). Outward currents of single hippocampal cells obtained from the adult guinea-pig. *Journal of Physiology* **393**, 331–353.

SEGAL, M. & BARKER, J. L. (1984). Rat hippocampal neurons in culture: potassium conductances. *Journal of Neurophysiology* **51**, 1409–1433.